Decellularized bovine reinforced vessels for small-diameter tissue-engineered vascular grafts

CLAUDIO GRANDI[1], SILVIA BAIGUERA[1], FRANCESCA MARTORINA[1], SILVANO LORA[2], PIETRO AMISTÀ[3], DANIELE DALZOPPO[1], COSTANTINO DEL GAUDIO[4], ALESSANDRA BIANCO[4], ROSA DI LIDDO[1], MARIA TERESA CONCONI[1] and PIER PAOLO PARNIGOTTO[1]

[1]Department of Pharmaceutical Sciences, University of Padova, I-35131 Padua; [2]Institute for Organic Synthesis and Photoreactivity, ISOF-CNR, I-40129 Bologna; [3]Department of NeuroRadiology, Hospital of Rovigo, I-45100 Rovigo; [4]Department of Chemical Sciences and Technologies, INSTM Research Unit, University 'Tor Vergata', I-00133 Rome, Italy

Received March 30, 2011; Accepted April 28, 2011

DOI: 10.3892/ijmm.2011.720

Abstract. The aim of the present study was to investigate the influence of a decellularization protocol on the structure and the mechanical behavior of small-diameter (<6 mm) tibial calf arteries and veins. Calf vessels were decellularized by a detergent-enzymatic method (DEM), partially hydrolyzed with trypsin and subsequently cross-linked using poly(ethylene glycol) diglycidyl ether. Our results showed that i) the DEM can be considered a simple and valuable procedure for the preparation of complete acellular arteries and veins able to preserve a high degree of collagen and elastic fibers, and ii) poly(ethylene glycol) diglycidyl ether cross-linking treatment provides appropriate mechanical reinforcement of blood vessels. Histologically, the decellularized vessels were obtained employing the detergent-enzymatic procedure and their native extracellular matrix histoarchitecture and components remained well preserved. Moreover, the decellularization protocol can be considered an effective method to remove HLA class I antigen expression from small-diameter tibial calf arteries and veins. Cytocompatibility of decellularized cross-linked vessels was evaluated by endothelial and smooth muscle cell seeding on luminal and adventitial vessel surfaces, respectively.

Introduction

To replace malfunctioning or diseased cardiovascular tissues, several reconstructive procedures have been developed with the aim of increasing implant biocompatibility, including the transfer of healthy tissue from one site or individual to another and the use of living tissue prosthetics obtained through the tissue engineering approach (1). Although successful with large diameter (>6 mm) high-flow vessels, autografts, allografts or synthetic prosthetic grafts can not meet clinical demand, especially in low-flow small-diameter vascular grafts (SDVGs) which are often connected with thrombosis, aneurysm formation, calcification, and severe inflammatory reactions (2). The vascular tissue engineering procedure is an innovative, multidisciplinary approach, which could be applied to creating completely biological and functional SDVGs. The SDVG must be biocompatible, non-thrombogenic, non-immunogenic, resistant to infection, with appropriate mechanical (such as ability to withstand long-term hemodynamic stress without failure) and physiological (such as compliance and appropriate vasoconstriction/relaxation responses) properties, together with an ease of handling and suturability (3). Currently, synthetic polymer scaffolds, cell sheets, hydrogels or biopolymer scaffolds and decellularized tissues are the main approaches that have been investigated and their advantages and disadvantages in obtaining functional SDVGs have been recently reviewed (3).

In the last few years, acellular matrices, containing extracellular matrix (ECM) proteins that serve as intrinsic templates for cell attachment and growth, have been successfully used in both pre-clinical animal studies and in human clinical applications (1,4). The goal of a decellularization protocol is to efficiently remove all cellular and nuclear material while minimizing any adverse effects on the composition, biological activity and mechanical integrity of the remaining ECM. Moreover, microscopic and ultrastructural features of the matrix play important roles in modulating cell adhesion and migration (5). The most commonly utilized approaches for tissue decellularization include a combination of physical, chemical and enzymatic treatments (6). Depending on the tissue from which ECM is harvested, each decellularization process could adversely impact the tissue to varying degrees. Physical treatments, such as sonication or freezing, damage ECM (7,8), chemical treatments with non-ionic (Triton X-100) or ionic (sodium dodecyl sulfate) detergents remove glycosaminoglycans from collagenous tissues (9,10), while enzymatic treatments decrease laminin, fibronectin and elastin content (11,12).

Correspondence to: Professor Claudio Grandi, Department of Pharmaceutical Sciences, University of Padua, Via Marzolo 5, I-35131 Padua, Italy
E-mail: claudio.grandi@unipd.it

Key words: small-diameter vascular graft, decellularization, cross-linking, extracellular matrix, tissue engineering

However, the ultrastructure and 3-D architecture of ECM scaffolds can be largely preserved throughout the processing required for tissue decellularization if care is taken to avoid harsh chaotropic agents.

Meezan *et al* developed a simple and easy detergent-enzymatic method (DEM), able to remove all cellular components, including major histocompatibility complex antigens responsible for immune response activation, without affecting matrix structural properties (5). Moreover, the basal membrane, which plays an important role in keeping selective permeability and tissue integrity, was also preserved (5). The DEM approach has been proven as an effective method to obtain ECM-derived prosthetic grafts, which can support *in vitro* and *in vivo* cell adhesion and proliferation: acellular matrices are remodelled in living tissues and can function as urethra (13), small bowel (14), skeletal muscle (15), esophagus (16) and tracheal (17) substitutes. However, while many studies focused on the decellularized tissue biocompatibility, cell seeding and implantation potential, only few reported findings on relationships between tissue decellularization and the physical and mechanical properties of tissue (7,18).

Taking these considerations into account, the present study evaluates the structural and mechanical properties as well as cell compatibility of acellular matrices obtained from small-diameter tibial calf (<6 mm) arteries and veins. Moreover, decellularized calf vessels were partially hydrolyzed with trypsin and subsequently cross-linked using the chemical cross-linking reagent, poly(ethylene glycol) diglycidyl ether (PDGE) in order to improve mechanical characteristics.

Materials and methods

Culture media and reagents. All chemicals and reagents were obtained from Sigma Chemical Co. (St. Louis, MO), except for phosphate-buffered saline (PBS) tablets (Gibco Invitrogen Corporation, Paisley, UK), sodium chloride (Fluka, Basel, Switzerland), Mayer's hemalum and Eosin Y solution (Merck, Darmstadt, Germany), the DAB peroxidase substrate kit, the Avidin/Biotin Blocking kit, the Universal quick kit Biotinylated pan-Specific antibody, the Vectastain ABC kit and the Vectashield Mounting medium for fluorescence with DAPI (Vector Laboratories, Burlingame, CA), the mouse monoclonal anti-HLA Class I [W6/32] antibody (Abcam, Cambrige, UK), Movat pentachromic stain (Diapath, Bergamo, Italy), endothelial cell growth medium MV2 and smooth muscle cell growth medium 2 (PromoCell, Heidelberg, Germany), and collagenase I (Roche, Basel, Switzerland).

Preparation of acellular vessels. Tibial arteries and veins (length about 10 cm, diameter <6 mm) were harvested from calves, put into cold PBS solution and kept at 4˚C during transport. On arrival at the laboratory, after the removal of blood and surrounding soft tissue, vessels were extensively washed with PBS solution containing 1% antibiotic and antimycotic solution. They were divided into two groups. The first group of vessels was decellularized. To remove the cellular part of the tissue, a modification to Meezan's method was applied (5). A single decellularization cycle consisted of 3 steps: i) treatment with distilled water for 72 h at 4˚C, ii) incubation in 4% sodium deoxycholate solution for 4 h at room temperature, and iii) after washing, treatment with 2000 KU (Kunitz Unit) DNase-I in 1 M NaCl for 2 h at room temperature. The decellularization protocol was repeated for the number of cycles necessary to obtain complete organ decellularization (4 DEM cycles). Samples were stored in PBS containing 1% antibiotic and antimycotic solution at 4˚C until use. The second group of vessels was decellularized using the procedure previously described but was also cross-linked. To obtain cross-linked scaffolds, after each decellularization cycle, the decellularized vessels were treated with 1 mg/ml trypsin in PBS for 10 min at 37˚C, and then with 1% PDGE for 1 h at 37˚C. Samples were then mounted on a stainless steel tube and left to dry overnight. To deactivate remaining epoxide groups, cross-linked vessels were treated with 1 M glycine for 24 h at 37˚C and washed four times (1 h for each) with deionized water. Eight subgroups containing at least three arteries and three veins in each group were obtained. The average outer diameter and wall thickness of arteries and veins of both groups were measured using a caliper and recorded.

Histological analysis. Native vessels and samples after each decellularization cycle were fixed for 24 h in 10% formalin solution in neutral PBS at room temperature. They were washed in distilled water, dehydrated in graded alcohol, embedded in paraffin and sectioned at 5 μm. Sections were stained with haematoxylin and eosin stain (H&E) to verify the presence of cellular elements and with Movat pentachromic staining to evaluate the extracellular matrix components. To quantify the amount of cells still visible after each cycle of DEM, 10 cryostat sections (5 μm thick) from each specimen were stained with DAPI. The total number of nuclei were counted at x250 using fluorescence microscopy (Leica DM2000, Leica Microsystems, Wetzlar, Germany). The cell density was expressed as the number of nuclei/10^5 μm^2.

Scanning electron microscopy (SEM). Native vessels, decellularized and cross-linked vessels after each decellularization cycle, and cell cultures on acellular vessels were fixed with 2.5% glutaraldehyde in 0.1 M cacodylate buffer (pH 7.2) overnight. After critical point drying and gold sputtering, samples were examined by a scanning electron microscope (Stereoscan-205 S; Cambridge Instruments, Cambridge, MA).

Immunohistochemistry. The presence of MHC-positive cells was verified at each cycle. Briefly, cryostat sections were fixed with acetone and aspecific sites were blocked with 10% horse serum in PBS for 45 min at room temperature. Samples were incubated at 37˚C for 1 h with monoclonal anti-HLA Class I [W6/32] antibody diluted at 1:250 in 3% horse serum in PBS. After incubation of 30 min at room temperature with the Biotinylated pan-Specific antibody, samples were treated with the Vectastain ABC kit and then a DAB peroxidase substrate kit. Samples were examined under an optical microscope (Leica DM2000). Negative controls were carried out by similarly treating cultures but omitting the primary antibody.

Mechanical testing. A uniaxial tensile test was performed on longitudinally cut vessels by means of a universal testing machine (Lloyd LRX, 100N load cell) at 5 mm/min until

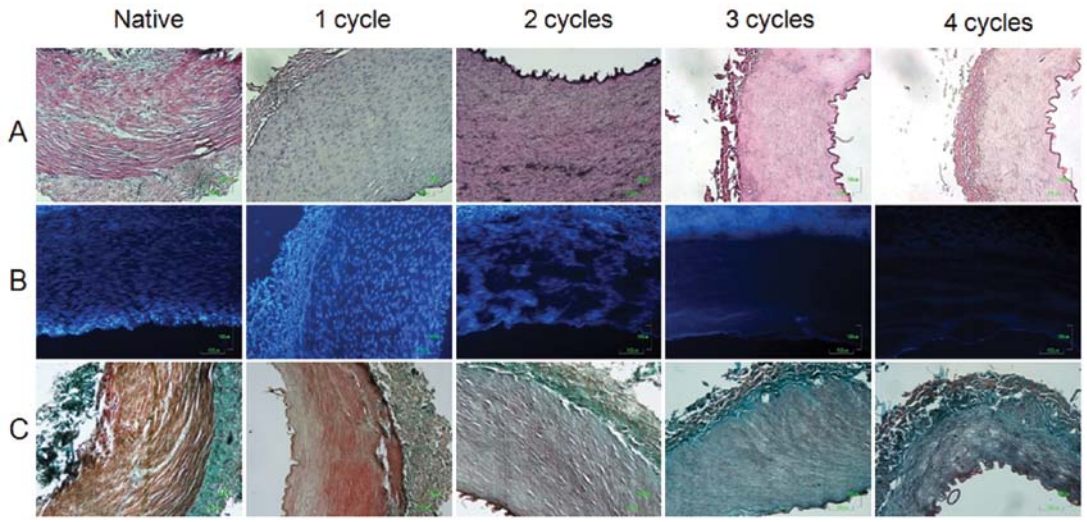

Figure 1. Histology of native and decellularized calf arteries. Cross-sections of native and decellularized arteries stained with (A) hematoxylin and eosin, (B) DAPI and (C) Movat's pentachrome (collagen, yellowish-orange; elastin, black; fibrins, light red; proteoglycans, blue; muscle layer, red). Magnification, x100.

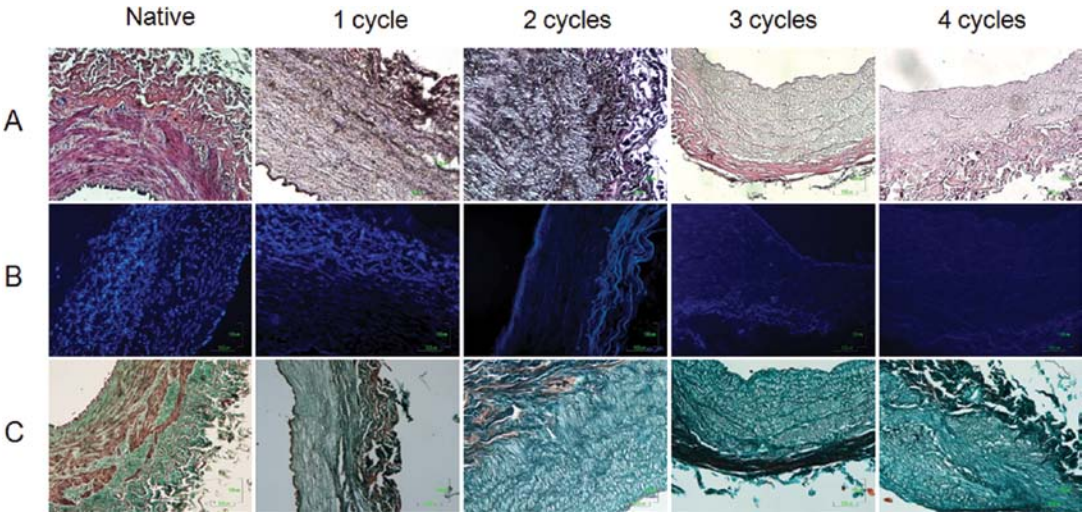

Figure 2. Histology of native and decellularized calf veins. Cross-sections of native and decellularized veins stained with (A) hematoxylin and eosin, (B) DAPI and (C) Movat's pentachrome (collagen, yellowish-orange; elastin, black; fibrins, light red; proteoglycans, blue; muscle layer, red). Magnification, x100.

rupture occurred (gripping distance 30 mm). Samples, kept in PBS solution containing 1% antibiotic and antimycotic solution, were mounted on the testing device with two grips cushioned with emery paper. Stress was defined as the tensile force divided by the initial cross-section area and the strain defined as the ratio between the grip displacement and the initial gripping distance (19). Because a blood vessel acts as a 'two-phase' material the tensile modulus at low (E1) and high (E2) strains were calculated by means of linear regression before and after the physiological range, being referred to elastin (low strain) and collagen (high strain) response, respectively (20). The tensile strength (TS) and deformation at break (ε_R) were also calculated (21).

Cell cultures on acellular vessels. HUVECs were isolated from human umbilical cords by collagenase digestion, as previously described (22), seeded on fibronectin (1 μg/cm^2)-coated dishes and cultured with endothelial cell growth medium MV2 supplemented with 5% fetal calf serum (FCS), 5 ng/ml epidermal growth factor (EGF), 0.2 μg/ml hydrocortisone, 0.5 ng/ml vascular endothelial growth factor, 10 ng/ml basic fibroblast growth factor (bFGF), 20 ng/ml R3 IGF-1 and 1 μg/ml ascorbic acid. HAoSMCs were obtained from Sigma and cultured according to the manufacturer's instructions using the smooth muscle cell growth medium 2 supplemented with 5% FCS, 0.5 ng/ml EGF, 2 ng/ml bFGF and 5 μg/ml insulin. Both HUVECs and HAoSMCs were used at passage 3. Decellularized and cross-linked vessels were sterilized in 80% ethanol for 4 h and left in PBS overnight. Using a microsyringe, HUVECs (4x10^5 cells/cm^2) and HAoSMCs (2.5x10^5 cell/cm^2) were seeded longitudinally onto the internal or external side of the samples, respectively. Every 30 min, vessels were rotated 90 degrees until all surfaces had been completely exposed to cells. The cells were maintained in culture under static conditions with their specific media (described above) for 7 days and then examined by SEM.

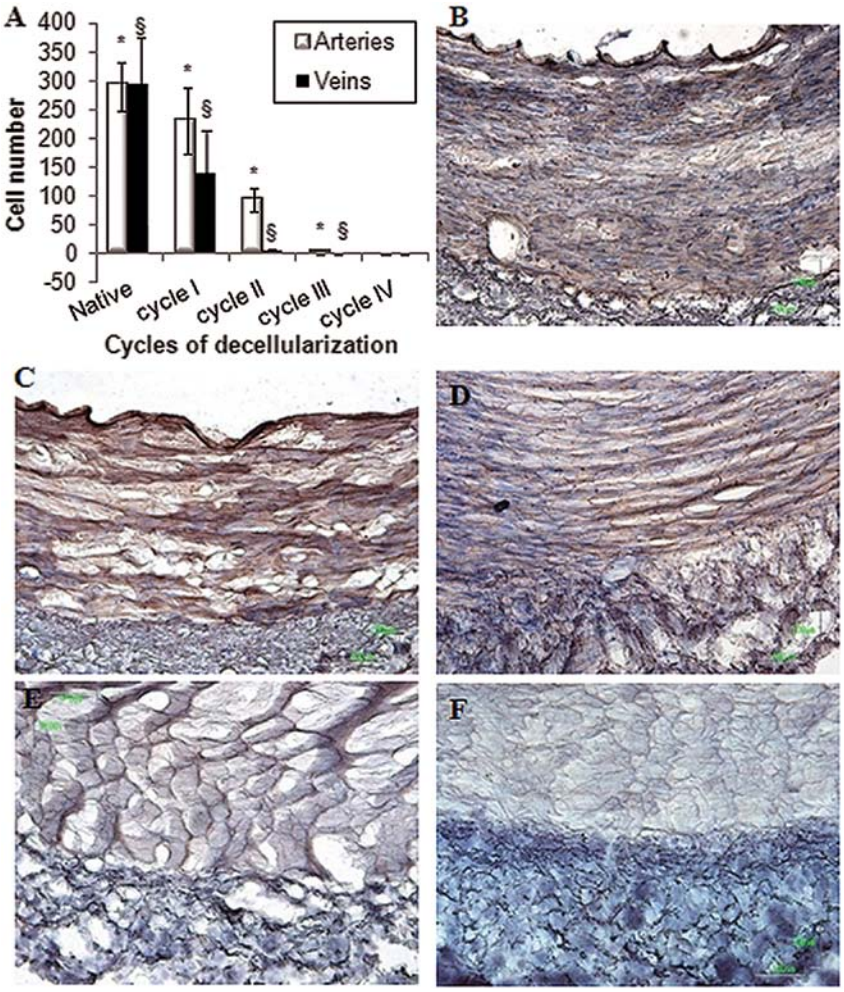

Figure 3. (A) Cell number of native and decellularized calf arteries (white bars) and veins (black bars). Results are expressed as mean ± SD. Significant differences ($^{§,*}P<0.05$) were detected among each DEM cycle for both arteries and veins. (B-F) Immunohistochemistry of (B) native and DEM-treated arteries after (C) 1, (D) 2, (E) 3 and (F) 4 cycles. Brown staining represents HLA class I. Magnification, x100.

Statistical analysis. Results are expressed as the mean ± SD of at least three different vessels. Statistical comparisons were performed by analysis of variance (ANOVA), followed by a t-test of a Student-Newman-Keuls post-hoc test.

Results

Morphological analysis of decellularized vessels. Tibial calf arteries and veins were completely decellularized using 4 DEM cycles. After each of the 4 cycles, ECM morphology and the degree of decellularization were evaluated by means of H&E, DAPI and Movat stainings. The histological sections of native and decellularized arteries and veins are presented in Figs. 1 and 2, respectively. Native vessels showed expected structural characteristics. In particular, arteries presented a more compact and muscular structure compared to veins, with a visible distinction between intimal, medial and adventitial layers, as demonstrated by Movat pentachromic staining (Figs. 1C and 2C). Arteries were more resistant to cell removal compared to veins. Indeed, decellularization of arteries occurred only after the 2nd cycle (Fig. 1A and B), whereas only one DEM cycle induced an almost complete disappearance of cellular elements in the veins (Fig. 2A and B). The DEM approach allowed the removal of cells from both types of vessels while preserving most ECM components, such as collagen and elastic laminae (Figs. 1C and 2C). Nevertheless, after the 3rd cycle, the adventitial layer of both veins and arteries appeared less compact and more extended compared to the respective native vessels. Furthermore, Movat staining revealed a progressive decrease of the muscular components of arteries from the 1st to the 4th DEM cycle. A complete loss of the muscular components was observed in veins after only the 1st DEM cycle (Figs. 1C and 2C). Complete decellularization was confirmed by cell nuclear counting. The plot reported in Fig. 3A showed a significant reduction of cell number between the 2nd and the 3rd DEM cycle in arteries ($P<0.05$) and between the 1st and the 2nd DEM cycle in veins ($P<0.05$). Four decellularization cycles were needed to completely remove HLA Class I antigen expression from arteries (Fig. 3B-F). Similar results were obtained with veins (data not shown). A diffuse immunoreactivity against HLA Class I was visible until the 2nd cycle, after that it decreased and no staining was visible at the end of DEM cycles.

Micrographs, reported in Figs. 4 and 5, showed the ECM ultrastructure of intimal and adventitial surfaces of arteries and veins, respectively. Based on previous histological results,

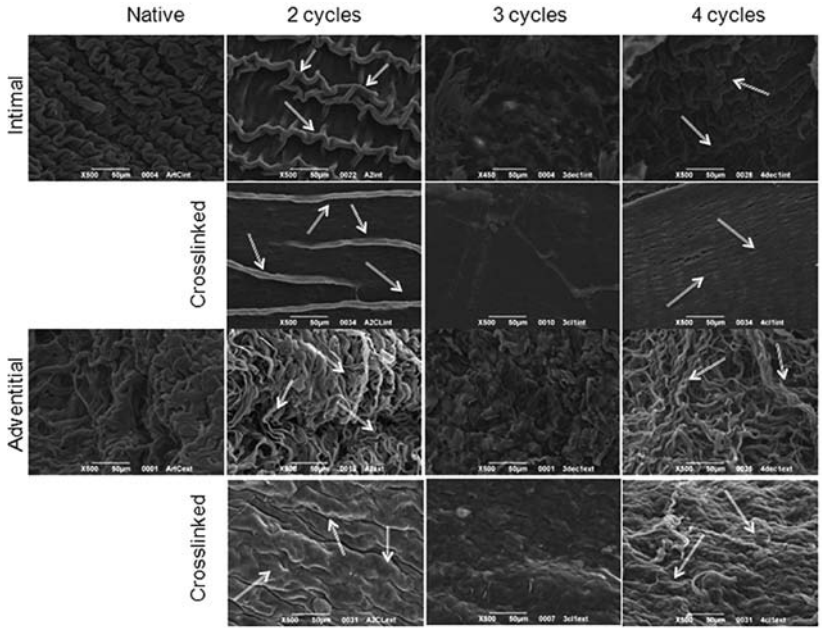

Figure 4. SEM micrographs of intimal and adventitial surfaces of native, decellularized and cross-linked arteries. In the intima of the native arteries, white arrows indicated a corrugated endothelial layer with exposed basement membrane underneath. In the adventitia, white arrows indicated collagen fibers which were crimped before cross-linking treatment and un-crimped after cross-linking treatment. Magnification, x500.

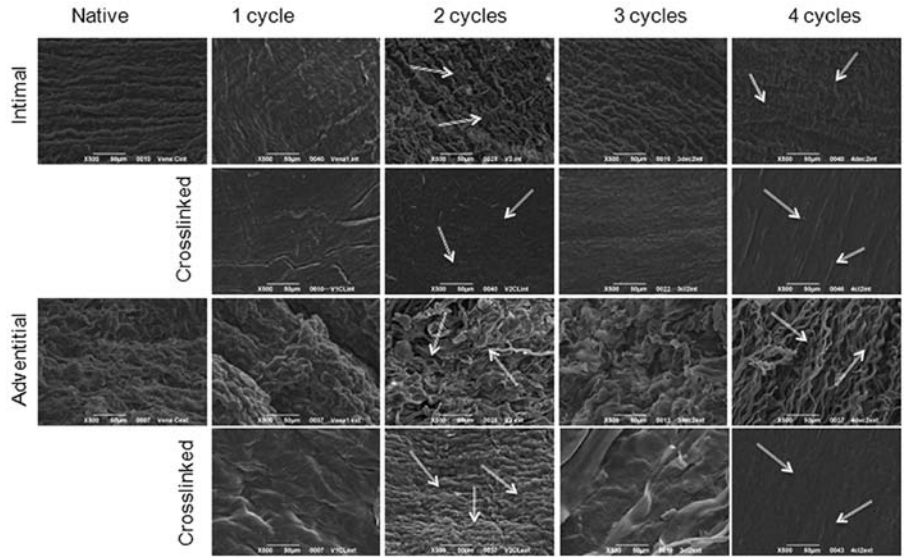

Figure 5. SEM micrographs of intimal and adventitial surfaces of native, decellularized and cross-linked veins. In the *intima* of the native veins, white arrows indicated an intact corrugated endothelial layer, which became stretched and smoother after decellularization and cross-linking treatment. In the adventitia, white arrows indicated thick bundles of crimped collagen fibers. Magnification, x500.

SEM observations of arteries concerned only samples treated from the 2nd decellularization cycle onwards. In native arteries and veins, an intact corrugated endothelial layer was visible on the surface of the intima, which became stretched and smoother after decellularization (Figs. 4 and 5, in arrows). The connective basal membrane was still visible in both vessels, even after all decellularization cycles. Regarding the adventitia, SEM observations confirmed the previous histological results: native samples showed the presence of thick bundles of crimped collagen fibers, which appeared to be fewer and un-crimped after decellularization (Figs. 4 and 5, in arrows). On the other side, fibers appeared to be intact suggesting that the decellularization protocol had not harshly damaged the ECM histoarchitecture. Macroscopic observations revealed that cross-linked vessels maintained a natural color and retained their cylindrical shape, while the decellularized samples were shown to be softer and less rigid. SEM micrographs of cross-linked vessels showed that PGDE treatment induced stretching and smoothing of vessel ECM ultrastructure (Figs. 4 and 5).

Diameter and thickness of vessels. The outer diameter and the wall thickness of all the investigated samples are presented in Fig. 6. Native arteries and veins showed comparable outer diameters (3.2±0.1 and 3.3±0.5 mm, respectively). After the

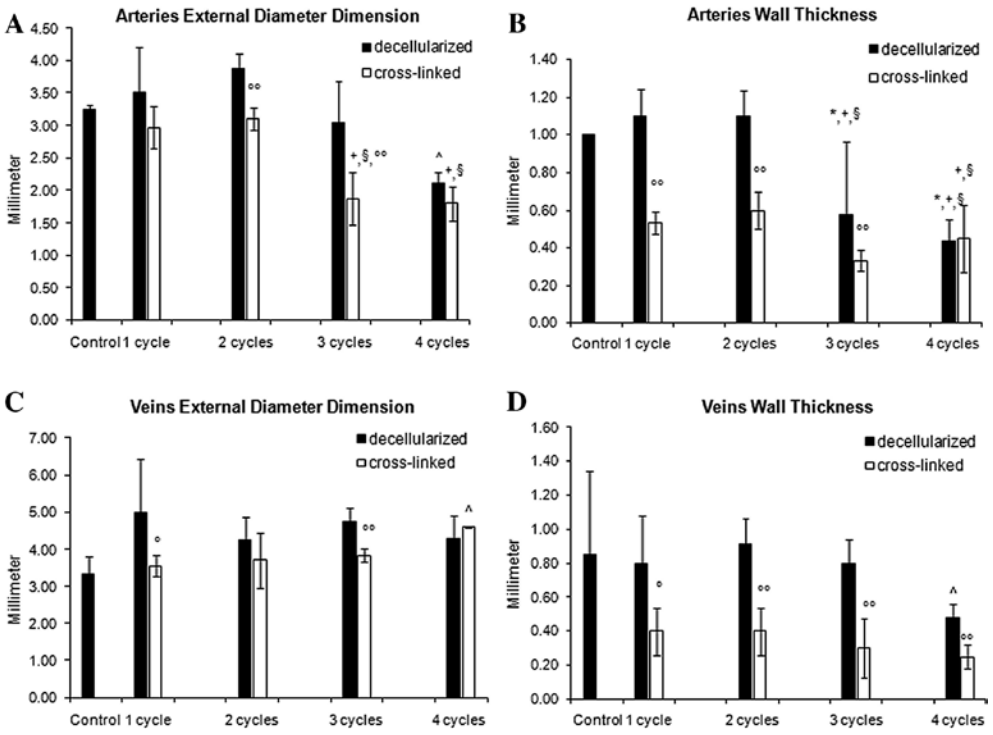

Figure 6. Physical characterization of decellularized and cross-linked calf (A and B) arteries and (C and D) veins. (A and C) Outer diameter and (B and D) wall-thickness measurements. *P<0.05 vs. control; +P<0.05 vs. 1st DEM cycle, §P<0.05 vs. 2nd DEM cycle; ^P<0.05 vs. all other vessels; °P<0.05 and °°P<0.001 vs. decellularized vessels.

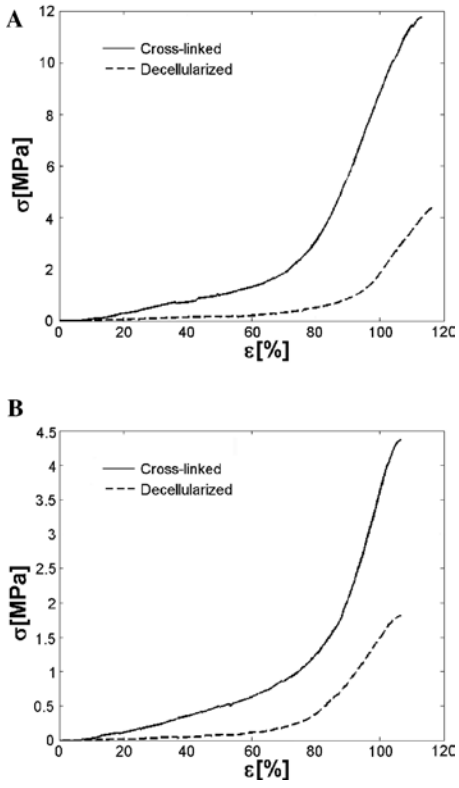

Figure 7. Stress-strain curve acquired in the uniaxial tensile test for calf (A) arteries and (B) veins.

1st and 2nd decellularization cycle, the outer diameter of arteries increased by 8 and 19%, respectively, compared to the native samples. The 3rd and the 4th decellularization cycles, instead, produced a significant (P<0.05) decreasing trend of the outer diameters of arteries (3.9±0.2 and 2.1±0.2 mm, respectively), which was 36% smaller compared to the native ones at the end of the 4th cycle (Fig. 6A). Regarding the veins, the outer diameter increased by 50% after the 1st decellularization cycle, and remained higher than the native veins also during the subsequent cycles ending with an increase of 28% after the 4th cycle (Fig. 6C). The cross-linking treatment induced a significant (P<0.05) decrease of the outer diameter of both vessel types with respect to the non-cross-linked ones (Fig. 6A and C). It should be pointed out that for veins a significant trend was observed only for samples treated from the 1st to the 3rd DEM cycles (Fig. 6C). As expected, native arteries showed an average wall thickness (1.0±0.1 mm) slightly higher than native veins (0.8±0.5 mm). With increasing decellularization cycles, vessel wall thickness showed a similar trend to that observed for the outer diameter. The wall thickness of cross-linked vessels showed a decrease of nearly 50% (P<0.05 and P<0.001, respectively for arteries and veins), with respect to non-cross-linked samples (Fig. 6B and D).

Mechanical testing. A stress-strain curve representative of the different behavior of cross-linked and non-cross-linked blood vessels for both arteries and veins is shown in Fig. 7. As expected, the mechanical resistance strongly increased after cross-linking. In arteries (Fig. 8), cross-linked vessels generally showed a significant increase in mechanical properties compared to the respective non-cross-linked samples, except for the deformation at break (P>0.05). E1 and E2 presented the maximum values after the 2nd DEM cycle, showing a decrease for the successive 3rd and 4th DEM cycles, even if not statistically significant (Fig. 8A and B). Comparable values

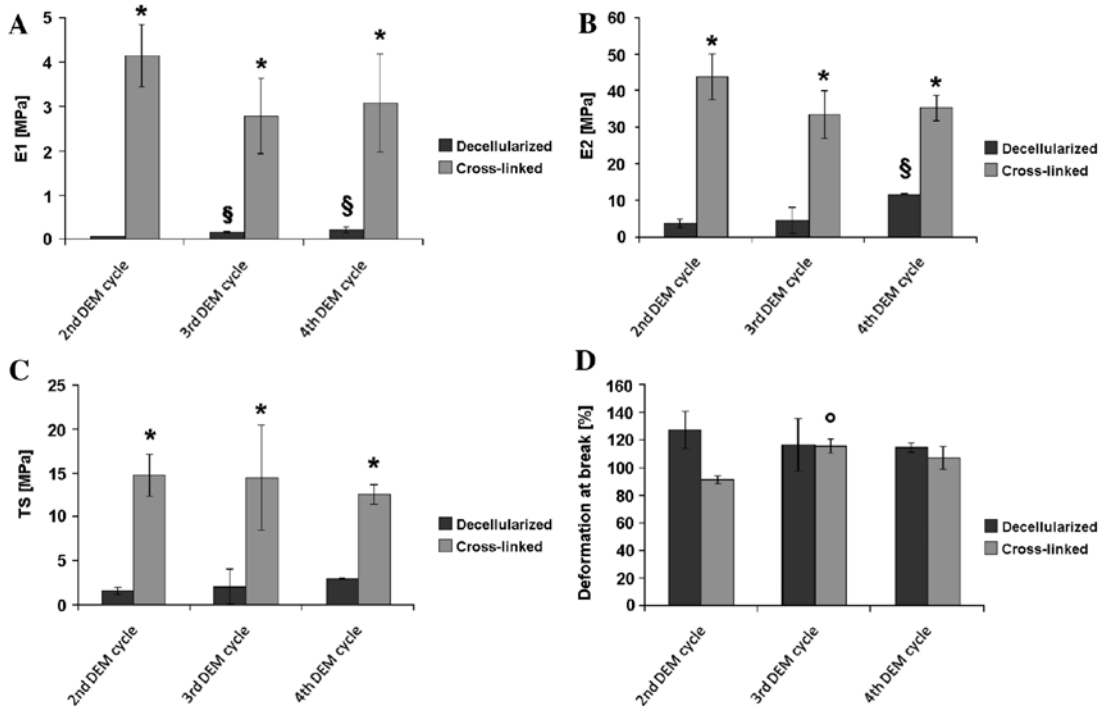

Figure 8. Mechanical characterization of decellularized and cross-linked calf arteries. (A) Tensile modulus at low strains, (B) tensile modulus at high strains, (C) tensile strength and (D) deformation at break. *P<0.05 decellularized vs. cross-linked vessels for each cycle; §P<0.05 of any DEM cycle vs. the 2nd DEM cycle; °P<0.05 any cross-linked DEM cycle vs. 2nd cross-linked DEM cycle.

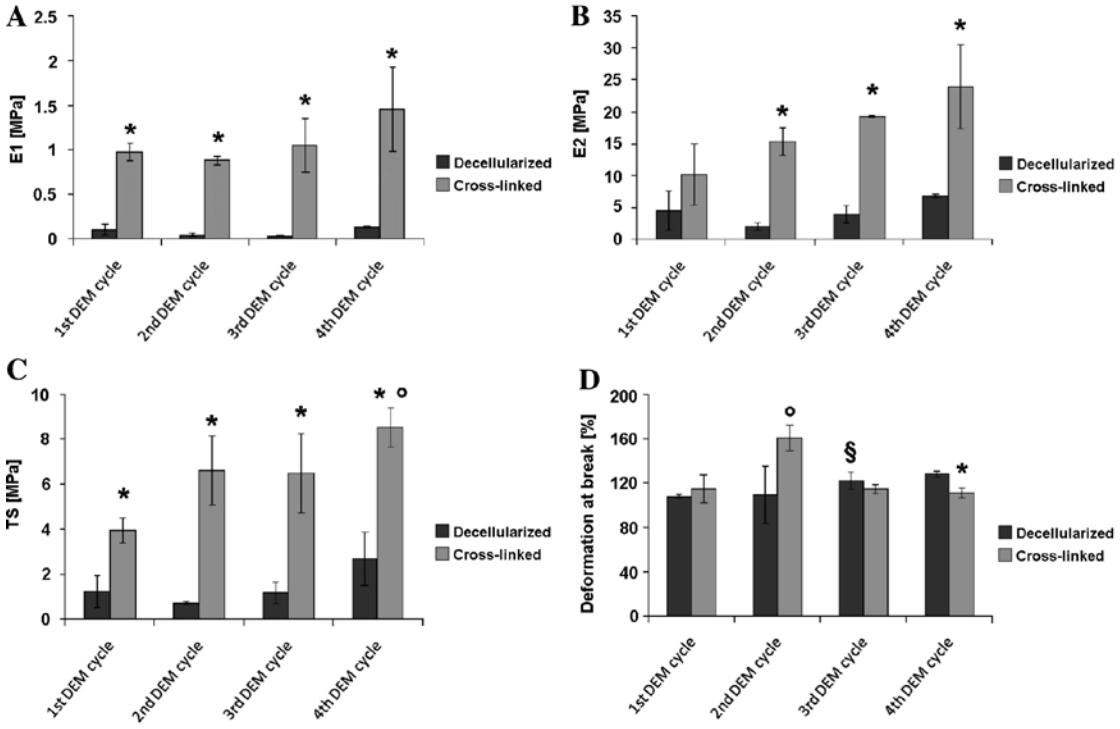

Figure 9. Mechanical characterization of decellularized and cross-linked calf veins. (A) Tensile modulus at low strains, (B) tensile modulus at high strains, (C) tensile strength and (D) deformation at break. *P<0.05 decellularized vs. cross-linked vessels for each cycle; §P<0.05 of any DEM cycle vs. 1st DEM cycle; °P<0.05 any cross-linked DEM cycle vs. 1st cross-linked DEM cycle.

were computed for the TS both for the decellularized and for the cross-linked arteries (Fig. 8C). The decellularization as well as the cross-linking process had little effect on the absolute values of the deformation at break of artery matrices (Fig. 8D). The mechanical properties of the veins were not significantly affected by progressive decellularization cycles (Fig. 9). Cross-linked veins, generally, showed significantly (P<0.05) increased mechanical characteristics compared to non-cross-linked

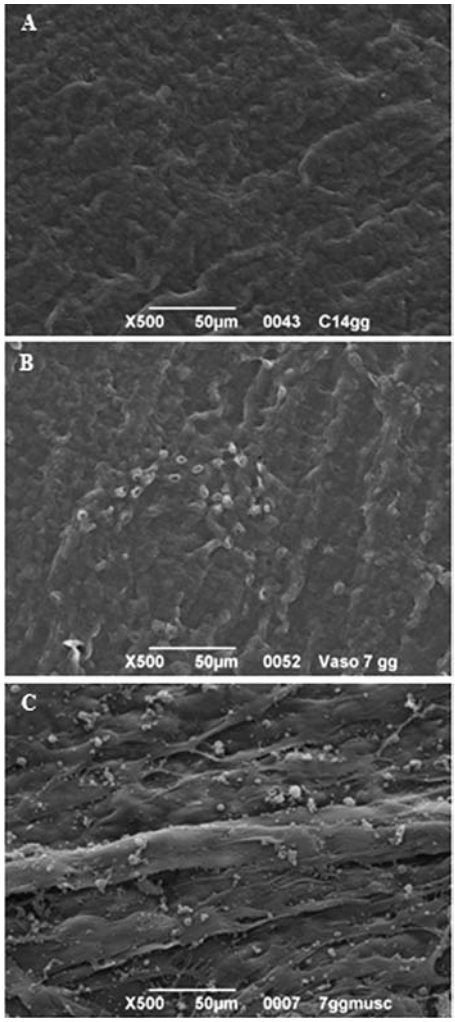

Figure 10. SEM micrographs of native cross-linked arteries with (A) no cells and after 7 days from (B) HUVECs or (C) HAoSMCs seeding. Magnification, x500.

samples, except for deformation at break. E1, E2 and TS showed an increasing trend starting from the 1st to the 4th DEM cycles, revealing the specific role of the cross-linking procedure.

Cytocompatibility of cross-linked vessels. HUVECs and HAoSMCs were seeded in static culture conditions on the intimal and adventitial sides of cross-linked arteries treated with 4 DEM cycles, respectively, and cultured for 7 days. The cross-linked vessels maintained their tubular shape and did not collapse during the entire culture period. Both HUVECs and HAoSMCs almost completely covered the culture surfaces (Fig. 10). Similar results were obtained with cross-linked veins (data not shown).

Discussion

The aim of the present study was to evaluate in which way subsequent DEM cycles can influence major ultrastructure, morphology and biomechanical properties of small-diameter tibial calf vessels and to relate structural changes to mechanical properties. Moreover, since decellularization efficiency is dependent on both tissue thickness and architecture (i.e. the resistance to solvent diffusivity increases for thicker samples or when a highly dense ECM is present) (23), both tibial calf arteries and veins were examined.

In arteries, cellular components (mostly smooth muscle cells) were retained after the first DEM cycle and complete cellular removal was achieved after the 2nd DEM cycle. Veins, however, were depleted of cells just after the 1st DEM cycle. Decellularization efficiency relies on the diffusion of the solvent throughout the sample. This diffusion is limited by the density and thickness of the ECM and the different response of arteries and veins is closely related to differences in vessel structure. As histological sections demonstrated, indeed, native calf arteries and veins presented the expected structural differences with arteries having a more compact structure and higher smooth muscle component, resulting in higher resistance to the decellularization treatment than veins.

Goissis *et al* (23) have previously demonstrated a different response of dog arteries and veins to the decellularization process; however, they obtained complete cellular removal on arteries only after extended alkali treatment, with a significant ECM degradation and reduction of collagen content. DEM, however, did not depend on the cycle number and did not profoundly alter the ECM morphology and histoarchitecture of the decellularized vessels, demonstrating that the three-dimensional structure of the ECM was significantly preserved. Considering that collagen is responsible for vessel strength and elastin for distensibility and recoil (24), these findings are very important in assessing the validity of this decellularization method to obtain a suitable ECM scaffold for constructing functional tissue-engineered SDVGs.

Indeed, it has been reported that human endothelial and muscular cells rapidly undergo programmed cell death in the absence of any ECM interaction (25), and that an intact ECM plays an important role not only in the maintenance of tissue structure and function, but also in the regulation of vascular cell migration, proliferation and survival (4,26,27). Moreover, histological and SEM analysis of decellularized vessels demonstrated the preservation of an intact luminal basement membrane (BM), after each DEM cycle. An intact BM can prevent *in vitro* cell penetration into the underlying matrix and foster the formation of confluent cell populations that cover the surface (4,28). Histological and SEM analysis of decellularized small-diameter vessels demonstrated the effectiveness of the DEM approach on decellularization of the tissue, preserving ECM structural components (even after 4 decellularization cycles) necessary for cell attachment and repopulation. On the other hand, HLA class I antigen expression gradually disappeared through DEM treatments and completely vanished after four cycles. Therefore, the DEM was demonstrated to be an effective method to remove HLA class I antigen expression from decellularized small-diameter tibial calf arteries and veins.

Vessel external diameter and wall thickness were affected by the different DEM cycles, with an initial increase and a progressive decrease with decellularization cycles, which was particularly evident in arteries. The biomechanical properties of vessels are related to the structural links between smooth muscle cells and ECM components (27). Certain expectations can be made regarding the physical and mechanical properties

of an ECM based on an understanding of its collagen fiber architecture (4). Even the collagen fiber of an ECM scaffold plays a critical role in determining its biomechanical behavior. It is then reasonable to assume that the variations observed are linked to the loss of muscular components caused by the decellularization process, explaining, at the same time, the major effect observed on arteries (composed of more muscular structures) in comparison with veins. Therefore, smooth muscle cell content is an important factor in determining the physical and biomechanical properties of vessels after decellularization (29).

The main problem related to naturally-derived tissues is their high rate of degradation *in vitro* and, as a consequence, appropriate pre-treatments are necessary to reduce biodegradation and antigenicity, to enhance the material resistance to enzymatic degradation, to stabilize tissue structure and to maintain mechanical properties (1).

Over the years, a number of cross-linking approaches (chemical, physical and biological) have been investigated (30); however, at present, there is not a commonly accepted ideal cross-linking treatment for collagen-derived bio-prosthesis. It has been recently reported that chemical stabilization through bifunctional agents (as epoxy compounds) leads to scaffolds that are characterized by thermal, structural, physical, and mechanical properties similar to those of native tissues (31). In this study, a polyepoxy compound, PGDE, was employed to cross-link decellularized vessels after each DEM cycle. PGDE is a hydrophilic cross-linking agent and its application to natural biomaterials may be more effective in overcoming some of the drawbacks that are typically encountered with glutaraldehyde. Glutaraldehyde reacts only with the ε-amino group of lysine residues in proteins, whereas polyepoxy compounds react with amino, carboxyl, phenol and alcohol groups (32,33). Moreover, the presence of a flexible long polyethylene glycol chain and the bifunctional nature of PGDE are able to cross-link structures less complex than those deriving from glutaraldehyde treatment (34). As a consequence, polyepoxy-treated vessels and valves have been shown to be softer, more flexible, and have shown better tolerance to natural strain compared to glutaraldehyde-treated tissue (35). Finally, it has been reported that polyepoxy treatment of cardiovascular tissues, due to the formation of a polyethylene glycol hydrogel layer, reduces tissue calcification and improves resistance to thrombosis and aneurysm (36). After all the DEM cycles, a short treatment with trypsin, adopted to increase the free amino group content, allowed PGDE to be more effective. These treatments had minor effects on the overall structure of both vessel types: intact intimal BM and adventitial un-crimped collagen fibers were still retained and the slight flattening of these structures is related to the intramolecular and intermolecular cross-linking which involve collagen fibrils. Moreover, cross-linking pre-treatment reduces the free volume in tissues, expelling some water molecules out of the fixed tissue, with a consequent reduction of the physical dimension of blood vessels, such as external diameters and wall thickness.

There was a significant increase in the biomechanical properties of cross-linked arteries compared to the related non-cross-linked samples. The former revealed maximum values after the 2nd DEM cycle with a subsequent decrease for the successive 3rd and 4th DEM cycles. This behavior can be ascribed to the presence of more abundant muscular components in the 1st and 2nd DEM cycle with respect to the two successive DEM cycles and to the resulting un-crimped collagen structure, as histologically observed. Referring to this latter point, it has been previously reported that decellularized rabbit carotid arteries were stiffer than native vessels, being probably related to the presence of un-crimped collagen in decellularized arteries (18). Therefore, it is possible to infer that both these conditions (i.e. variation of muscular structures and presence of un-crimped collagen fibers) can contribute to the enhancement of the mechanical properties of the arteries, especially considering that the more exposed altered collagen structure offers more reactive functional sites, increasing the cross-linking efficiency and the strength of vessels.

Other experiments on arteries have shown these vessels to be nonlinear, anisotropic and viscoelastic, confirming our data. Vito and Dixon (37) provided a thorough review of the constitutive models developed for arteries, classifying their behavior as viscoelastic, pseudoelastic or poroelastic due to the alignment of artery collagen fibers, also visible for our decellularized arteries. Conversely, decellularized veins were not characterized by significant changes in their mechanical properties, from the 1st to the 4th DEM cycle. This response can be related to no substantial modifications occurring after the 1st DEM cycle, suggesting that collagen mainly affected the mechanics of the vessels and that the slight differences observed for the computed parameters can be related to the intrinsic inter-variability of the samples themselves.

Generally, native veins are considered 'more compliant' than native arteries. Arteries have thicker walls than veins and contain more smooth muscle tissue and elastin. The thinner walls of veins contain a larger amount of inextensible collagen, but are more distensible than arterial walls due to their thinness (38,39). A report (40) on elastomechanical properties of native bovine veins showed a J-shaped behavior typical of collagenous materials, similar to the behavior found in our decellularized and cross-linked vessels. The longitudinal E1 of native bovine veins (0.1±0.02 MPa) reported by Rossmann (40) is comparable to our E1 values of decellularized (0.1±0.06 MPa) and cross-linked (0.98±0.1 MPa) bovine veins. Moreover, the longitudinal TS of decellularized (1.2±0.7 MPa) and cross-linked (3.9±0.6 MPa) bovine veins produced higher results than the native veins value (0.5±0.1 MPa) reported by Rossmann (40), indicating an increased collagen fiber strength. Therefore, decellularized and mostly cross-linked veins showed significantly increased mechanical characteristics with respect to the non-cross-linked ones. This result is related to the structural modification induced by the repeated decellularization processes that led the collagen to shift from thick bundles of crimped fiber configuration to un-crimped. We noticed an increase in the mechanical properties of arteries and therefore it would not be unreasonable to assume that their specific structure allows them to be linked by more functional sites. As a concluding remark, the deformation at break did not reveal significant variations either for arteries or veins after each decellularization cycle and the relative cross-linking process. This suggested that the proposed protocol did not modify the ultimate strain of the blood vessels under the conditions employed herein. A similar result has been previously reported investigating the mechanics of arterial tissue stored

in several conditions, showing that the ultimate strain of the treated samples did not differ from the control case (41).

Herein, we demonstrated that PGDE cross-linking of vessels subjected to different DEM cycles influenced the mechanical response and that PGDE, creating linear cross-linking within the collagenous matrices of decellularized vessels, allows for the production of SDVGs with appreciable mechanical strength. Even if less than glutaraldehyde, a cytotoxic effect related to the use of PGDE, as cross-linking agent, has been reported and attributed to the continuous release of unreacted PGDE still trapped within tissues and causing cellular death (42). It has been demonstrated that unreacted PGDE could be removed from the scaffolds by repeating the soaking steps in deionized water (43) and that the epoxide groups of unreacted PGDE within tissues could be deactivated by reaction with amino groups containing compounds, with a marked increase of cellular compatibilities of PGDE-fixed vascular tissue (44).

In the present study, cross-linked vessels were treated with a glycine solution and subsequently extensively washed. We reported that HUVECs and HAoSMCs adhered to and proliferated on, respectively, the luminal and adventitial surface of decellularized and cross-linked vessels. After 7 days, both HUVECs and HAoSMCs covered the vessel surfaces, indicating that our PGDE cross-linked vessels present good cell compatibility.

In conclusion, our results show that the DEM can be a simple and valuable approach for the preparation of complete acellular arteries and veins with a high degree of collagen, elastic fibers and BM preservation. The results of the mechanical properties showed that PGDE cross-linking treatment may provide appropriate mechanical reinforcement of blood vessels. The PGDE treatment allows both endothelial and muscular cell adhesion and proliferation on luminal and adventitial vessel surfaces, respectively. Moreover, the cross-linking of arteries and veins at different number of DEM cycles allows to obtain SDVGs with different size, thickness and mechanical properties.

Acknowledgements

The authors wish to thank Dr C. Furlan (Centro Universitario Grandi Apparecchiature Scientifiche-CUGAS-University of Padova) for SEM analysis.

References

1. Schmidt CE and Baier JM: Acellular vascular tissues: natural biomaterials for tissue repair and tissue engineering. Biomaterials 21: 2215-2231, 2000.
2. Teebken OE and Haverich A: Tissue engineering of small diameter vascular grafts. Eur J Vasc Endovasc Surg 23: 475-485, 2002.
3. Isenberg BC, Williams C and Tranquillo RT: Small-diameter artificial arteries engineered in vitro. Circ Res 98: 25-35, 2006.
4. Badylak SF, Freytes DO and Gilbert TW: Extracellular matrix as a biological scaffold material: structure and function. Acta Biomater 5: 1-13, 2009.
5. Meezan E, Hjelle JT and Brendel K: A simple, versatile, non disruptive method for the isolation of morphologically and chemically pure basement membranes from several tissues. Life Sci 17: 1721-1732, 1975.
6. Gilbert TW, Sellaro TL and Badylak SF: Decellularization of tissues and organs. Biomaterials 27: 3675-3683, 2006.
7. Dahl SL, Koh J, Prabhakar V and Niklason LE: Decellularized native and engineered arterial scaffolds for transplantation. Cell Transplant 12: 659-666, 2003.
8. Schenke-Layland K, Vasilevski O, Opitz F, Konig K, Riemann I, Halbhuber KJ, Wahlers T, and Stocka UA: Impact of decellularization of xenogeneic tissue on extracellular matrix integrity for tissue engineering of heart valves. J Struct Biol 143: 201-208, 2003.
9. Rieder E, Kasimir MT, Silberhumer G, Seebacher G, Wolner E and Simon P: Decellularization protocols of porcine heart valves differ importantly in efficiency of cell removal and susceptibility of the matrix to recellularization with human vascular cells. J Thorac Cardiovasc Surg 127: 399-405, 2004.
10. Hudson TW, Liu SY and Schmidt CE: Engineering an improved acellular nerve graft via optimized chemical processing. Tissue Eng 10: 1346-1358, 2004.
11. Courtman DW, Pereira CA, Kashef V, McComb D, Lee JM and Wilson GJ: Development of a pericardial acellular matrix biomaterial: biochemical and mechanical effects of cell extraction. J Biomed Mater Res 28: 655-666, 1994.
12. Bader A, Schilling T, Teebken OE, Brandes G, Herden T and Steinhoff G: Tissue engineering of heart valves-human endothelial cell seeding of detergent acellularized porcine valves. Eur J Cardiothorac Surg 14: 279-284, 1998.
13. Parnigotto PP, Gamba PG, Conconi MT and Midrio P: Experimental defect in rabbit urethra repaired with acellular aortic matrix. Urol Res 28: 46-51, 2000.
14. Parnigotto PP, Marzaro M, Artusi T, Perrino G and Conconi MT: Short bowel syndrome: experimental approach to increase intestinal surface in rats by gastric homologous acellular matrix. J Pediatr Surg 35: 1304-1308, 2000.
15. Conconi MT, De Coppi P, Bellini S, Zara G, Sabatti M, Marzaro M, Zanon GF, Gamba PG, Parnigotto PP and Nussdorfer GG: Homologous muscle acellular matrix seeded with autologous myoblasts as a tissue-engineering approach to abdominal wall-defect repair. Biomaterials 26: 2567-2574, 2005.
16. Marzaro M, Vigolo S, Oselladore B, Conconi MT, Ribatt D, Giuliani S, Nico B, Perrino G, Nussdorfer GG and Parnigotto PP: In vitro and in vivo proposal of an artificial esophagus. J Biomed Mater Res A 77: 795-801, 2006.
17. Macchiarini P, Jungebluth P, Go T, Asnaghi MA, Rees LE, Cogan TA, Dodson A, Martorell J, Bellini S, Parnigotto PP, Dickinson SC, Hollander AP, Mantero S, Conconi MT and Birchall MA: Clinical transplantation of a tissue-engineered airway. Lancet 372: 2023-2030, 2008.
18. Williams C, Liao J, Joyce EM, Wang B, Leach JB, Sacks MS and Wong JY: Altered structural and mechanical properties in decellularized rabbit carotid arteries. Acta Biomater 5: 993-1005, 2009.
19. Stemper BD, Yoganandan N and Pintar FA: Methodology to study intimal failure mechanics in human internal carotid arteries. J Biomech 38: 2491-2496, 2005.
20. Wagenseil JE and Mecham RP: Vascular extracellular matrix and arterial mechanics. Physiol Rev 89: 957-989, 2009.
21. Monson KL, Goldsmith W, Barbaro NM and Manley GT: Significance of source and size in the mechanical response of human cerebral blood vessels. J Biomech 38: 737-744, 2005.
22. Jaffe EA, Nachman RL, Becker CG and Minck CR: Culture of human endothelial cells derived from umbilical veins. Identification by morphologic and immunologic criteria. J Clin Invest 52: 2745-2756, 1973.
23. Goissis G, Suzigan S, Parreira DR, Maniglia JV, Braile DM and Raymundo S: Preparation and characterization of collagen-elastin matrices from blood vessels intended as small diameter vascular grafts. Artif Organs 24: 217-223, 2000.
24. Douglas JF, Gaughran ER, Henderson J, Lord GH and Rosenberg N: The use of arterial implants prepared by enzymatic modification of arterial heterografts. II. The physical properties of the elastica and collagen components of the arterial wall. AMA Arch Surg 74: 89-95, 1957.
25. Meredith JE, Fazeli B and Schwartz MA: The extracellular matrix as a cell survival factor. Mol Biol Cell 4: 953-961, 1993.
26. Newby AC and Zaltsman AB: Molecular mechanisms in intimal hyperplasia. J Pathol 190: 300-309, 2000.
27. Raines EW: The extracellular matrix can regulate vascular cell migration, proliferation, and survival: relationships to vascular disease. Int J Exp Pathol 81: 173-182, 2000.
28. Brown B, Lindberg K, Reing J, Stolz DB and Badylak SF: The basement membrane component of biologic scaffolds derived from extracellular matrix. Tissue Eng 12: 519-526, 2006.

29. Roy S, Silacci P and Stergiopulos N: Biomechanical properties of decellularized porcine common carotid arteries. Am J Physiol Heart Circ Physiol 289: H1567-H1576, 2005.
30. Rault I, Frei V, Herbage D, Abdul-Malak N and Huc A: Evaluation of different chemical methods for cross-linking collagen gel, films and sponges. J Mater Sci Mater Med 7: 215-221, 1996.
31. Zeugolis DI, Paul GR and Attenburrow G: Cross-linking of extruded collagen fibers: a biomimetic three-dimensional scaffold for tissue engineering applications. J Biomed Mater Res A 89: 895-908, 2009.
32. Shecter L and Wynstra J: Glycidyl ether reactions with alcohols, phenols, carboxylic acids, and acid anhydrides. Ind Eng Chem 48: 86-93, 1956.
33. Tu R, Quijano RC, Lu CL, Shen S, Wang E, Hata C and Lin D: A preliminary study of the fixation mechanism of collagen reaction with a polyepoxy fixative. Int J Artif Organs 16: 537-544, 1993.
34. Lee JM, Pereira CA and Kan LW: Effect of molecular structure of poly(glycidyl ether) reagents on crosslinking and mechanical properties of bovine pericardial xenograft materials. J Biomed Mater Res 28: 981-992, 1994.
35. Zhou J, Quintero LJ, Helmus MN, Lee C and Kafesjian R: Porcine aortic wall flexibility. Fresh vs Denacol fixed vs glutaraldehyde fixed. ASAIO J 43: M470-M475, 1997.
36. Tomizawa Y, Noishiki Y, Okoshi T and Koyanagi H: Development of a small-caliber vascular graft with antithrombogenicity induced by extreme hydrophilicity. ASAIO Trans 34: 644-650, 1988.
37. Vito RP and Dixon SA: Blood vessels costitutive models-1995-2002. Annu Rev Biomed Eng 5: 413-439, 2003.
38. Jacot JG, Abdullah I, Belkin M, Gerhard-Herman M, Gaccione P, Polak JF, Donaldson MC, Whittemore AD and Conte MS: Early adaptation of human lower extremity vein grafts: wall stiffness changes accompany geometric remodeling. J Vasc Surg 39: 547-555, 2004.
39. Bank AJ, Wang H, Holte JE, Mullen K, Shammas R and Kubo SH: Contribution of collagen, elastin, and smooth muscle to in vivo human brachial artery wall stress and elastic modulus. Circulation 94: 3263-3270, 1996.
40. Rossmann JS: Elastomechanical properties of bovine veins. J Mech Behav Biomed Mater 3: 210-215, 2010.
41. Stemper BD, Yoganandan N, Stineman MR, Gennarelli TA, Baisden JL and Pintar FA: Mechanics of fresh, refrigerated, and frozen arterial tissue. J Surg Res 139: 236-242, 2007.
42. Nishi C, Nakajima N and Ikada Y: In vitro evaluation of cytotoxicity of diepoxy compounds used for biomaterial modification. J Biomed Mater Res 29: 829-834, 1995.
43. Min S, Gao X, Liu L, Tian L, Zhu L, Zhang H and Yao J: Fabrication and characterization of porous tubular silk fibroin scaffolds. J Biomater Sci Polym Ed 20: 1961-1974, 2009.
44. Yu XX, Wan CX and Chen HQ: Preparation and endothelialization of decellularised vascular scaffold for tissue-engineered blood vessel. J Mater Sci Mater Med 19: 319-326, 2008.